Title

CD8 follicular T cells localize throughout the follicle during germinal center reactions and maintain cytolytic and helper properties

Authors

Valentine, Kristen M
Mullins, Genevieve N
Davalos, Oscar A
et al.

Publication Date

2021-09-01

DOI

10.1016/j.jaut.2021.102690

Peer reviewed

HHS Public Access

Author manuscript

J Autoimmun. Author manuscript; available in PMC 2022 August 12.

Published in final edited form as:

J Autoimmun. 2021 September ; 123: 102690. doi:10.1016/j.jaut.2021.102690.

CD8 follicular T cells localize throughout the follicle during germinal center reactions and maintain cytolytic and helper properties

Kristen M. Valentine[a,d], **Genevieve N. Mullins**[a,d], **Oscar A. Davalos**[a], **Lek Wei Seow**[b], **Katrina K. Hoyer**[a,b,c]

[a]Quantitative and Systems Biology Graduate Program, University of California Merced, Merced, CA 95343

[b]Department of Molecular and Cell Biology, School of Natural Sciences, University of California Merced, Merced, CA 95343

[c]Health Sciences Research Institute, University of California Merced, Merced, CA 95343

Abstract

Follicular CXCR5+ PD-1+ CD8 T cells (CD8 Tfc) arise in multiple models of systemic autoimmunity yet their functional contribution to disease remains in debate. Here we define the follicular localization and functional interactions of CD8 Tfc with B cells during autoimmune disease. The absence of functional T regulatory cells in autoimmunity allows for CD8 Tfc development that then expands with lymphoproliferation. CD8 Tfc are identifiable within the lymph nodes and spleen during systemic autoimmunity, but not during tissue-restricted autoimmune disease. Autoimmune CD8 Tfc cells are polyfunctional, producing helper cytokines IL-21, IL-4, and IFNγ while maintaining cytolytic proteins CD107a, granzyme B, and TNF. During autoimmune disease, IL-2-KO CD8 T cells infiltrate the B cell follicle and germinal center, including the dark zone, and in vitro induce activation-induced cytidine deaminase in naïve B cells via IL-4 secretion. CD8 Tfc represent a unique CD8 T cell population with a diverse effector cytokine repertoire that can contribute to pathogenic autoimmune B cell response.

Keywords

CD8 T follicular cells; CXCR5+ CD8 T cell; autoimmunity; germinal center; T regulatory cell

Corresponding author: Dr. Katrina K. Hoyer, Molecular and Cell Biology, University of California Merced, 5200 N. Lake Rd., CA 95343. Phone: 209-228-4229; Fax: 209-228-4060; khoyer2@ucmerced.edu.

[d]contributed equally

Author contributions: KMV; conceptualization, formal analysis, original draft writing, experimental investigation and visualized figures, GNM; experimental investigation, formal analysis, original draft writing, OAD; formal analysis and experimental investigation, original draft writing. LWS; formal analysis, KKH; conceptualization, original draft writing, visualization, funding acquisition, and supervision.

Conflict-of-interest disclosure: The authors have declared that no conflict of interest exists.

1. Introduction

CXCR5+ CD8 T cells arise during situations of chronic antigen and inflammation including models of chronic viral infection, multiple cancer types, and antibody mediated autoimmune disease (1–3). In some conditions CXCR5 expression facilitates CXCR5+ CD8 T cell homing to CXCL13 expressed in B cell follicles while other studies find that the persistent expression of CCR7 on CXCR5+ CD8 T cells prevents follicle entry (4–7). Irrespective of disease, CXCR5+ CD8 T cells express the transcriptional repressor Bcl-6 that is associated with CD8 T effector memory differentiation and CXCR5 expression (7–16). CXCR5+ CD8 T cells also demonstrate a gene profile associated with Bcl-6 function including TCF-1, E2A, and E-protein related family members Id2 and Id3 expression (13, 17). Despite recent research that explores CXCR5+ CD8 T cells, variance in tissue localization, expression profiles, inflammatory conditions, and developmental stages limit comparisons between studies.

Functionally, CXCR5+ CD8 T cells respond in an antigen specific manner. In situations of chronic viral infection CXCR5+ CD8 T cells maintain an effector memory phenotype, capable of reseeding the CD8 T cell niche and controlling viral infection (7, 13). CXCR5+ CD8 T cells isolated from patients with colon cancer promote antibody mediated immune responses, whereas cells isolated from hepatocellular carcinoma promote antibody mediated immune responses and exhibit cytolytic capacity towards tumor cells (9, 18, 19). CXCR5+ CD8 T cells generated during inflammation also maintain cytolytic function (5). In the context of autoimmunity, we have previously shown that a subset of CXCR5+ CD8 T cells that also co-express PD-1, localize to the germinal center and mediate antibody class switching (10). Despite the emergence of comprehensive and robust research, a consistent description of CXCR5+ CD8 T cell development and function remains elusive.

As the priming cues for CXCR5+ CD8 T cells are similar to those for CD4 T follicular helper (Tfh) cells, the recruitment and entry of CXCR5+ CD8 T cells into the follicle and germinal center are likely also similar (3). CD4 Tfh entry into the germinal center begins upon antigen encounter and migration to the T-B border. Once there, interactions with B cells re-enforce key migratory protein expression, such as CXCR5 upregulation and CCR7 downregulation, which progresses as the CD4 Tfh cells move first into the follicle and then the germinal center (20). Once in the germinal center, CD4 Tfh and CXCR5+ CD8 T cells interact via cell:cell contact and cytokine secretion to influence B cell differentiation, antibody class switch and memory (21). The interaction between self-reactive CXCR5+ CD8 T cells or CD4 Tfh cells and self-reactive B cells that arise during autoimmune disease may promote disease.

Here we show that autoimmune CXCR5+PD-1+ CD8 T cells (CD8 Tfc) develop with inflammation and the absence of T regulatory (Treg) cells regardless of IL-2 availability. Similar to data described for CXCR5+ CD8 T cells in viral infection and cancer, CD8 Tfc maintain cytolytic capacity while, within the germinal center, CD8 Tfc employ multiple cytokine and direct cell:cell mechanisms to manipulate B cell responses. These data provide further evidence that CD8 Tfc development requires exposure to chronic antigen and perhaps chronic inflammation to promote autoimmune disease progression.

2. Methods

2.1. Mice, antibody depletions, and immunizations.

BALB/c IL-2 knockout (KO), CD25 (IL-2Rα)-KO, IL-2.IFNγ-double KO (dKO), and IL-2.CD28-dKO were used with littermate IL-2 wildtype or heterozygous (WT) controls (22, 23). IL-2 mediated autoimmune disease is not gender specific such that only age is used to determine disease and is indicated for each experiment. CD4 or CD8 depletions were performed in WT and IL-2-KO mice by 5 intraperitoneal (i.p.) injections from day 8–16 of age with 20 μg anti-CD4 (GK1.5; BioXcell) or anti-CD8 (2.43; BioXcell) antibody per gram weight. BALB/c hemizygous male Foxp3sf/Y (scurfy) mice and HET female FoxPsf/+ (scurfy-HET) littermate controls were used as previously described (10). Scurfy and scurfy-HET mice were depleted of IL-2 by 5 i.p. injections from day 7–16 of age using 20 μg/g mouse of anti-IL-2 (JES6-1A12; BioXcell) or PBS (Omega). Male scurfy mutant containing IL-2-KO (scurfyxIl-2) mice were generated by crossing scurfy heterozygous, IL-2 heterozygous females to IL-2-heteozyogous scurfy WT males for F1 progeny that contained both scurfy and IL-2-KO. MRL/MpJ-*Fas*^{lpr}/J (Mrl.lpr) mice were purchased from Jackson Laboratory (JAX000485) and MRL.MpJ mice, as controls for Mrl.lpr mice, aged 17 weeks or more were generously donated by Dr. Gabriela Loots at Lawrence Livermore National Laboratory. Non-obese Diabetic (NOD) mice generously donated by Dr. Hans Dooms at Boston University were used at 11 weeks of age after urine testing as glucose positive. Collagen-induced arthritis mice were generated as described (24) using 6–8-week-old C57BL/6 mice (JAX000664) injected intradermally with 100 μg type II chicken collagen in complete Freund's adjuvant (CFA) containing 200 μg tuberculosis mycobacterium supplemented by a collagen boost of 50 μg type II chicken collagen in incomplete Freund's adjuvant (IFA). B6N.129-*Il21r*^{tm1Kopf}/J (IL-21R-KO mice; JAX019115) were used to isolate B cells. All mice were housed and bred in specific-pathogen free conditions in accordance with UC Merced's Department of Animal Research Services and approved by the UC Merced Institutional Animal Care and Use Committee.

2.2. Flow cytometry and cell sorting.

All antibodies were purchased from eBioscience at Fisher Scientific unless otherwise specified. Lymphocytes and/or splenocytes were processed and stained in 1% fetal bovine serum (FBS; Omega) phosphate buffered saline (PBS; Omega). Splenocyte red blood cell (RBC) lysis was performed in 3 mL of 1x ammonium chloride lysis buffer for 1 min at room temperature (RT). CXCR5+ PD-1+ CD4 Tfh or CD8 Tfc were identified as previously described (10). In brief, lymphocytes and splenocytes were stained first for CXCR5-biotin (SPRCL5) for 1 hour at RT, then stained for CD4 (RM4-5), CD8 (53-6.7), PD-1 (Biolegend; J43), ICOS (C398.4A), fixable viability 506, streptavidin (SA; BD Biosciences), CD11c (N418), CD11b (M1/70), Ly6G (Gr-1; RB6-8C5), and B220 (RA3-6B2) for 30 min at 4°C. CD4 Tfh and CD8 Tfc are described as live CXCR5^{+}PD-1^{+}B220^{-}CD11c^{-}CD11b^{-}GR-1^{-} and were gated by fluorescence minus one for CXCR5+PD-1+ cells. Non CD4 Tfh and Non CD8 Tfc were determined as CXCR5-PD-1-. CD8 Tfc cells were evaluated for Treg markers by staining with CD122 (TM-b1), CD44 (IM7), and ICOSL (HK5.3) or were fixed after CD8 Tfc surface staining with the FoxP3 fixation/permeabilization kit (Thermofisher/Invitrogen) following manufacturer instructions for intracellular staining then stained with

Foxp3 (FJK-16s) and Helios (22F6). To assess B cell expression of activation induced deaminase (AID), cultured cells were surface stained for B220, CD19 (6D5), and viability dye 506 for 30 min at 4°C. Cells were then fixed using the FoxP3 fixation/permeabilization kit prior to intracellular staining for AID (mAID-2) and fluorochrome-conjugated SA for 45 min at RT for each.

To isolate CD4 Tfh and CD8 Tfc, splenocytes and lymphocytes were processed and negatively selected for T cells using a murine PE-selection kit (Stem Cell Technologies) using CD11c, CD11b, Ly6G (Gr-1) and B220 in PE. T cells were then stained for CXCR5 and PD-1 and sorted at greater than 85% purity. Naïve WT or IL-21R-KO B cells were isolated from splenocytes by staining for CD19, TCRβ (H57-597), CD11c, CD11b, Gr-1 and fixable viability dye 506 for 30 min at 4°C. B cells were sorted at greater than 95% purity. All flow cytometry and cell sorting were performed on Becton Dickinson LSR-II and BD Biosciences Aria II cell sorter, respectively. Flow cytometric analysis was performed using FCS Express with Diva Version 4.07.005 (DeNovo Software) or FlowJo Version 10.1 (FlowJo).

2.3. T cell stimulations.

Processed cells were stimulated with 50 ng/ml phorbol 12-myristate 13-acetate (PMA) and 500 ng/ml ionomycin with brefeldin A (BFA) for 5 hours at 37°C and 5% CO_2. Post-stimulation staining was categorized into multiple panels. For all panels cells were surface stained with follicular cell markers above except SA, then fixed using the Foxp3 fixation and permeabilization kit and stained for intracellular cytokines. In panel 1, CD8 Tfc were stained with SA, perforin (eBioOMAK-D), granzyme B (NGZB), and IFNγ (XMG1.2) or SA, granzyme B and IFNγ for 45 minutes at RT. In panel 2, CD8 Tfc were stained tertiarily with IL-21R-chimeria for 1 hour at RT then with SA, IL-10 (JES5-16E3), IL-4 (11B11), and IL-21R (eBio4A9) for 45 minutes at RT. In panel 3, CD8 Tfc follicular cells were stained tertiarily with IL-21R-chimeria for 1 hour at RT then with SA, IL-21R, and IFNγ for 45 minutes at RT. To stain for CD107a (eBio1D4B), 5 μl in 200 μl stimuli was used during the 5-hour stimulation without BFA for the first hour.

2.4. In vitro T cell and B cell culture assays.

Indirect co-culture of T and B cells by supernatant was performed as described previously (10). In brief, FACS isolated T cell populations were plated at 5×10^4 cells per well and activated with 5 μg/mL soluble anti-CD3ε (17A2; BioXCell) and 1 μg/mL soluble anti-CD28 (37.51; BioLegend) for 72 hours. Supernatant from activated T cells was plated with 5×10^4 sorted WT or IL-21R-KO B cells per well and with 1 μg/ml anti-CD40 (IC10) and 5 μg/ml F(ab')2 goat anti-mouse IgMμ (Jackson ImmunoResearch Laboratories) for 3 days for assessment of AID expression or 6 days for assessment of B cell antibody production by ELISA as described (10). For IL-4 depleted co-culture, T cells were plated with stimuli and 2 μg/mL anti-IL-4 (11B11) for 72 hours.

2.5. RNA isolation and analysis of RNA next generation sequencing.

RNA sequencing (RNAseq) of 4 IL-2-KO CD8 T cell samples are available at NCBI GEO (accession number GSE112540) and as previously published (10). IL-2-KO CD4 and CD8

Tfc cells were sorted from at least 6 pooled 15–16-day old lymph node and spleens. Samples were quick frozen and shipped to Expression Analysis for total RNA isolation and TruSeq stranded mRNA sequencing. Four samples were sequenced with 2 biological replicates each for IL-2-KO CD4 Tfh and IL-2-KO CD8 Tfc. Quality and adapter content of raw reads were analyzed using FastQC (version 0.11.8). Adapter removal and quality trimming were performed using trimmomatic (version 0.38) (25). Read pairs were mapped to the patch assembly (C57BL/6J) of GRCm38/mm10 NCBI build 38.p6 (GCF_000001635.26) using Rsubread (version 1.34.7) with default settings (26). Gene level read count summarization was performed using featureCounts which used a modified version of the GRCm38/mm10 annotation containing only protein coding genes (27). Multi-mapping reads were counted without use of fractional counts when mapping to several genes, reads mapping across more than one gene. Genes with less than one count per million in at least three samples were removed. To account for varying sequencing depths, read counts were normalized using trimmed mean of M-values (TMM) in edgeR (version 3.26.8) (28). Read counts were transformed using the voomWithQualityWeights function for differential expression analysis in limma (version 3.40.6) (29–31). Genes were considered differentially expressed if their p-value was less than 0.05 after adjusting for false positive rate using Benjamini-Hochberg correction (32). Heatmaps were generated with log2 count per million (log-CPM) using package pheatmap (version 1.0.12) (33). Expression (log-CPM) of IL-2-KO CD8 Tfc and IL-2-KO CD4 Tfh expression was merged with prior RNAseq of day 12 IL-2-KO CD8 T cells and generated a heatmap to visualize gene expression differences (GSE112540) (10). Comparisons were conducted between IL-2-KO CD8 Tfc and IL-2-KO CD4 Tfh. Differentially expressed genes were annotated with their biological process using enrichGO from clusterProfiler (version 3.12.0) using the org.Mm.eg.db (version 3.8.2) database (34, 35). All analysis for read mapping, summarization, and differential expression analysis were performed using R versions v3.5.1 and v3.6.0 (36). Tidyverse (version 1.2.1) functions were used throughout the analysis for plotting and data wrangling (37).

2.6. Microscopy and Immunofluorescence.

Spleens from day 18–21 IL-2-KO, WT, and 6–8-week-old immunized WT mice 7-days post-keyhole limpet hemocyanin (KLH) with IFA immunization were collected and frozen in OCT. 10 μm sections were sliced from spleens on a Leica CM1860 cryostat. Sections were fixed in ice-cold acetone prior to staining. For chemokine receptor staining, CXCR5 (2G8, BD Biosciences) was performed as a 3-step stain (38), CXCR4 (SPRCL5, Invitrogen) as a 2-step stain (39), and CD4 (GK1.5, Invitrogen) or CD8β (eBioH35–17.2, Invitrogen), IgD (11–26C, Invitrogen), and PNA (Vector Laboratories) as a one-step 30 min stain. For cytokine staining, IL-4 (11B11, BD Bioscience) was performed as a 3-step stain (40), IL-21 (149204, R&D Systems) as a 2-step stain (38), and CD4 or CD8β, IgD, and PNA (Sigma-Aldrich) as a one-step 30 min stain. After staining, slides were treated with Fluoromount G (Southern Biotech) before a glass coverslip was applied. The sections were visualized with a Zeiss LSM 880 confocal system. Images were taken at 10x (10x/0.45 Plan Apochromat; 420640-9900) and 40x (40x/1.2 LC LCI Plan Apochromat; 420862-9970-799) objectives. Images were saved in three ways: 1) all 5 color channels; 2) only CD4/CD8, IgD, and PNA; and 3) CD4/CD8, CXCR5 or IL-4, and CXCR4 or IL-21. The latter two were used for counting analysis.

Before counting, all images were assigned blinded names and counted independently by two individuals and averaged to determine final counts. Images were counted in ImageJ (version 1.52a) using the cell counter plugin. Outlines around germinal centers were drawn using the polygon tool and determined by PNA+IgD- areas. T cells (either CD4 or CD8) were counted first, then presence of other markers (CXCR4, CXCR5, IL-4, or IL-21) on counted cells was determined. Cells were defined by round shapes with clear CD4 or CD8 staining along the outer edge with no staining on the interior. Cells were considered positive for surface markers if the stain was present along the outer edge of the cell. Cells were positive for cytokine if stain was present either on the cell edge and/or as puncta of stain on the interior.

2.7. Statistics.

All statistics, except for RNAseq, were performed on GraphPad Prism (Version 8.0.0). Differences between two means was assessed by Student's t-test with a Welsh correction if indicated. Differences between multiple groups was performed by ordinary 1-way or 2-way ANOVA with a Bonferroni correction. ELISA protein concentrations from a standard protein curve were interpolated using a sigmoidal four parameter logistic standard curve analysis. Statistical measurements were indicated in each figure legend and described as NS= not significant, * $p<0.05$, ** $p<0.01$, or *** $p\leq0.001$.

3. Results

3.1. CD8 Tfc arise in multiple models of autoimmune disease.

Recent variability in the functional role of CXCR5+ CD8 T cells may be attributed to differences in nomenclature and potential subpopulations, thus we sought to understand CXCR5+ CD8 T cell function as it relates to PD-1 co-expression. During severe autoimmune disease, IL-2-KO CD4 and CD8 T cells have similar total CXCR5+ T cell frequencies, 7.32% and 6.4% respectively. Yet, when compared to CXCR5+ CD4 T cells, CD8 T cells have reduced CXCR5+ CD8 T cell total numbers. IL-2-KO CXCR5+PD-1+ CD4 Tfh cells comprise 50% of the total CXCR5+ CD4 T cell population while IL-2-KO CXCR5+PD-1+ CD8 T cells (here termed T follicular cells [Tfc]) comprise only 37% of total CXCR5+ CD8 T cells (Supp Fig. 1A). These, IL-2-KO CD8 Tfc express more ICOS costimulatory molecules (Supp Fig. 1B) and Bcl-6 transcription factor (Supp. Fig. 1C) than their IL-2-KO CXCR5+PD-1- CD8 T cell, IL-2-KO CXCR5-PD-1- CD8 T cell (non Tfc), and WT naïve CD8 T cell counterparts. Specific analysis of the PD-1+ subset of CXCR5+CD8 T cells (CXCR5+PD-1+ CD8 Tfc versus CXCR5+ CD8 T cells) may explain reported differences in function and development between disease models and cell subsets.

CD8 Tfc function in response to systemic autoantigen may drive antibody production to exacerbate autoimmune disease. To determine which autoimmune conditions facilitate CD8 Tfc responses, we assessed models of systemic and tissue-specific autoimmunity. As previously determined, IL-2-KO and scurfy CD8 Tfc frequency and total numbers were elevated when compared to WT naïve mice (Fig. 1) (10). Autoimmunity in Fas^{lpr} mice presents as severe lymphoproliferation and antibody-mediated systemic lupus erythematosus (SLE) that is associated with an expanded Tfh population (41). During SLE in Fas^{lpr} mice splenic CD8 Tfc are also expanded, if less than CD4 Tfh, by frequency and total number

when compared to aged MRL.MpJ control mice (Fig. 1). However, when we assessed tissue-specific models of autoimmunity, non-obese diabetic (NOD) and collagen induced arthritis (CIA), CD8 Tfc did not arise despite a detectable CD4 Tfh population in the spleen (Fig 1A, B). It is possible that CD8 Tfc may instead be restricted to ectopic germinal centers or draining lymph nodes during tissue-specific autoimmunity although we did not detect CD8 Tfc in the draining lymph nodes of NOD or CIA mouse models (Fig 1C). Together these data suggest that CD8 Tfc predominately arise in response to systemic antigen and expand by lymphoproliferation to impact autoantibody responses.

3.2 CD8 Tfc have distinct germinal center populations in systemic autoimmunity.

CD4 Tfh can function in the extrafollicular region to influence plasma cell development (42) and within the germinal center during B cell cycling and somatic hypermutation (43). To determine if CD8 Tfc can similarly promote regionalized B cell responses during autoimmune disease, we sought to understand CD8 Tfc localization in and around the B cell follicle. Extrafollicular CD4 T cells express increased CXCR4 and decreased CCR7. Further license to enter the germinal center requires the addition of CXCR5 and decreased CXCR4 (39, 44). We first evaluated CXCR4 and CCR7 expression on IL-2-KO CD8 Tfc by flow cytometry. Unlike WT CD8 T cells (59.98 +/−9.08% CCR7+) or IL-2-KO CD8 non Tfc (58.16 +/−15.5% CCR7+) only a small population of CCR7+ CD8 Tfc exist (11.89 +/−10.51% CCR7+) (Fig. 2A). Instead, IL-2-KO CD8 Tfc have significantly higher frequency of CCR7- cells, of which, 58% are CXCR4- and 29% are CXCR4+, significantly more than observed in IL-2-KO non Tfc or WT naive CD8 T cells. The dominance of CD8 Tfc populations that express less CXCR4 and CCR7 suggest CXCR5+ is used to enter the light zone of the germinal center, while another CXCR4+CXCR5+ population likely populates the extrafollicular space (Fig. 2B).

To further determine CD8 Tfc localization within the tissue structure, we used immunohistochemistry to evaluate germinal centers, defined by PNA and IgD staining, during intermediate to late disease in IL-2-KO mice or in KLH-immunized WT controls (Fig 2C, Supp. Fig 2A). As expected, germinal centers and follicles in KLH-immunized WT mice contained no CD8 T cells (Supp Fig 2B) (10). The IL-2-KO mice had a significantly greater total number of CD4 T cells (1012.86 +/−364.55 per mm^2, 1046.39 +/−340.0 per mm^2) than CD8 T cells (168.90 +/−259.53 per mm^2, 421.06 +/−173.61 per mm^2) when normalized to the GC and follicle area. Of the CD8 T cells counted, an equal number of CD8 T cells were identified within the follicle and the GC area, similar to observations in CD4 T cell counts (Fig 2D). When germinal center IL-2-KO CD4 T cells were evaluated based on CXCR5 and CXCR4 expression, cells were split between CXCR5 expression alone (25.58 +/−20.63%) and no expression (47.02 +/−25.80%) (Fig 2E). In contrast, CD8 T cells tended to co-express more CXCR5 and CXCR4 (86.28 +/−18.01%) than CXCR4 (3.13 +/−8.84%) or CXCR5 (2.95 +/−5.48%) alone. This was also true of follicular localized CD8 T cells, although more follicular localized CD8 T cells expressed CXCR5 (12.98 +/−14.55%) or CXCR4 (22.87 +/−16.33%) alone than their germinal center localized counterparts (Fig 2F). Differences between confocal and flow results may be explained by the fact that CXCR5+ PD-1+ CD8 Tfc cells and CXCR5+ PD-1- CD8 T cells are separately evaluated in flow cytometry but are indistinguishable in the imaging data. These data suggest that CD8

T cells, like CD4 T cells, are capable of localizing to the B cell follicle and germinal center. The high co-expression of CXCR5 and CXCR4 on germinal center CD8 T cells suggests that CD8 T cells may localize preferentially to the dark zone of the germinal center, rather than the light zone where CD4 T follicular helper cells generally reside.

3.3. T cell regulation and not inflammation control CD8 Tfc differentiation.

CD4 T cell responsiveness to IL-2 dictates CD4 Tfh development (45, 46). To begin interrogating how IL-2 deficiency and Treg cell function influence CD8 Tfc development, we manipulated IL-2 availability in IL-2-sufficient, Treg-deficient scurfy mice (10). We first depleted IL-2 in scurfy mice using anti-IL-2 antibodies. Splenocytes from scurfy depleted of IL-2 maintain a similar CD8 Tfc frequency (1.3+/−0.71%) to untreated scurfy controls (0.6+/−0.15%), both of which are significantly reduced in comparison to IL-2-KO mice (Fig 3A). Then, to determine if germline IL-2 deficiency plays a greater role in CD8 Tfc development, we generated scurfy and IL-2-KO mice (scurfyxIL-2 mice). ScurfyxIL-2 splenocytes have slightly elevated CD8 Tfc compared to scurfy CD8 Tfc, yet scurfy CD8 Tfc (0.6+/−0.15%) and scurfyxIL-2 CD8 Tfc (6.01+/−2.71%) are significantly reduced in comparison to IL-2-KO CD8 Tfc (5.45+/−3.75%) (Fig. 3B). Further, the total number of splenocytes in scurfy and scurfy depleted of IL-2 but not scurfyxIL-2 mice were reduced compared to IL-2-KO mice (Fig 3C). The splenic CD8 Tfc expansion in IL-2-KO or scurfyxIl-2-KO mice compared to scurfy mice is likely due to differences in lymphoproliferation (47).

To explore if the lymphoproliferation accompanying IL-2 deficiency regulates CD8 Tfc expansion through CD28 co-stimulatory signals (48) and/or IFNγ-mediated feedback on CD8 T cell expansion (49), we assessed lymphopenic IL-2.CD28 dKO and lymphoproliferative IL-2.IFNγ dKO mice. Splenic CD8 Tfc frequency is significantly reduced in IL-2.CD28 dKO (0.59+/−0.26%) and IL-2.IFNγ dKO (1.3+/−0.56%) at late-stage disease (12 weeks) relative to IL-2-KO (3.5+/−1.2%) late-stage disease (3 weeks). However, the total number of splenic CD8 Tfc cells was slightly elevated in IL-2-KO and IL-2.IFNγ dKO spleens but not significantly different from IL-2.CD28 dKO even though the total splenocyte number was not significantly different between groups (Figure 3D). Further, in the absence of co-stimulation by CD28 or IFNγ signaling, the frequency of CD8 Tfc is significantly reduced compared to IL-2-KO mice suggesting that dysfunctional T cell activation or regulation may drive autoimmune CD8 Tfc development and expansion during autoimmune disease, as has been observed for CD4 Tfh (48, 49).

To test the possible influence of paracrine T cell interactions we depleted IL-2-KO mice of either CD4 or CD8 T cells before disease onset and evaluated CD4 Tfh or CD8 Tfc development at late-stage disease for PBS-treated IL-2-KO control mice. The frequency of IL-2-KO CD4 Tfh or CXCR5+PD-1^{lo} CD4+ does not change in the absence of total CD8 T cells. However, in the absence of CD4 T cells (including CD4 Tfh, activated T cells and remaining Tregs) CD8 Tfc (1.3+/−0.87%), are significantly reduced compared to untreated IL-2-KO CD8 Tfc (4.43+/−3.1%) (Figure 3E). Further suggesting that unstable or dysfunctional CD4 Treg, CD4 T follicular regulatory cells (Tfreg) and/or CD4 T effectors may drive CD8 Tfc development during autoimmune disease.

However, this CD8 Tfc population likely does not arise from unstable Foxp3+ Treg or Qa-1 restricted CD8 Treg populations previously defined in autoimmune disease (50, 51). CD8 Tfc do not express Foxp3, although a significant population of CD8 Tfc express Helios compared to non CD8 Tfc (Suppl Figure 3A). Helios expression is required for stable Treg and CD8 Qa-1-specific Treg to function but is also a marker of T cell activation and proliferation (52, 53). CD8 Tfc cells do not express ICOSL despite significantly elevated CD122 and CD44 co-expression (Suppl Figure 3B), suggesting that Helios expression by CD8 Tfc is an indication of activation rather than Treg differentiation. These data suggest that CD8 Tfc development is likely due to the absence of functional Tregs allowing for excessive T co-stimulation and signaling within the B cell follicle and enhanced by the absence of IL-2 signaling. CD8 Tfc cells then continue to expand during situations of lymphoproliferation promoted by IL-2 deficiency.

3.4. CD8 Tfc cell transcriptional expression indicates cytotoxic and B cell helper functionality, and a memory-like profile.

In autoimmune disease CD8 Tfc upregulate genes associated with a CD4 Tfh phenotype (10) but is also distinct from both naïve CD8 T and CXCR5- CD8 T cell transcriptional profiles (7). To determine how closely autoimmune CD8 Tfc resemble CD4 Tfh we performed RNAseq on day 15–16 lymph node and splenic IL-2-KO CD4 Tfh and IL-2-KO CD8 Tfc. Differential expression analysis identified 1118 genes (479 upregulated; 639 downregulated) that are differentially expressed between CD4 Tfh and CD8 Tfc (Figure 4A). IL-2-KO CD8 Tfc upregulated T cell activation genes *Sema4a*, *Crtam, Tnfsf4*, and CD8 effector genes *Ctsw*, *Nkg7*, *Klrd1*, and *Perf1* (Figure 4A). In line with trends observed in gene expression, differential gene expression categorized by gene ontology indicate cytokine production, cell:cell adhesion, and T cell activation as top biological processes eluding to dynamic IL-2-KO CD8 Tfc function (Figure 4B).

To further evaluate CD8 Tfc functional capacity we compared IL-2-KO CD4 Tfh and CD8 Tfc expression for known select genes associated with CD4 Tfh and CD8 effector T cells. As an exploratory comparison, we added our prior RNAseq of IL-2-KO day 12 CD8 T cells (GSE112540) (Figure 4C) (10). IL-2-KO CD8 Tfc upregulate genes associated with CD4 Tfh, including *Icos*, *Bcl-6*, and *Cd28*, especially when assessed against IL-2-KO total CD8 T cells. CD4 Tfh-associated genes are upregulated in IL-2-KO CD8 Tfc but are expressed at lower levels than in IL-2-KO CD4 Tfh, suggesting that IL-2-KO CD8 Tfc may not function as efficiently as traditional CD4 Tfh but may instead maintain diverse functional capacity (10). In fact, *Vdr*, *Sosdc1*, *Il21*, and *Cd40lg* expression is lower in IL-2-KO CD8 Tfc relative to IL-2-KO CD4 Tfh. In contrast to CXCR5+ CD8 T cells identified in chronic viral infection, IL-2-KO CD8 Tfc maintain effector gene expression via upregulated *Perf1* but not *Gzmb* or *Ctla4* compared to IL-2-KO CD4 Tfh cells. IL-2-KO CD8 Tfc and chronic viral CXCR5+ CD8 T cells upregulate exhaustion markers such as *Lag3*, *Havcr2 (Tim3)* and *Cd160* (7). Strikingly both IL-2-KO CD8 Tfc and CD4 Tfh express this exhaustion pattern suggesting a potential feedback mechanism for slowing antibody production during autoimmune disease. Together these data demonstrate that CD8 Tfc cells maintain a unique transcriptional profile incorporating CD4 Tfh and cytotoxic CD8 T cell gene patterns permitting diverse functional potential.

3.5. CD8 Tfc maintain diverse functional capacity.

In chronic viral infection and some cancer settings CXCR5+CD8 T cells maintain the capacity for cytolytic function by perforin and granzyme B protein expression (4, 54, 55). Our RNAseq analysis reveals that IL-2-KO CD8 Tfc transcriptionally express cytolytic genes so we investigated whether CD8 Tfc have cytolytic capacity during autoimmune disease. We examined the production of CD107a, granzyme B, perforin, and TNFα. A significantly higher frequency of IL-2-KO CD8 Tfc produce CD107a, granzyme B, perforin, and TNFα than IL-2-KO CD8 non Tfc. (Fig. 5A). IL-2-KO CD8 Tfc are more likely to be polyfunctional producing two or more cytolytic proteins (57.39% double; 5.46% triple) than IL-2-KO CD8 non Tfc (13.96% double; 0.43% triple) (Fig. 5B). IL-2-KO CD8 Tfc co-produce granzyme B and IFNγ (9.80%) or IFNγ and TNFα (47.0%), but some produce granzyme B (1.34%), IFNγ (25.8%) or TNFα (2.45%) alone (Figure 5B). Thus, individual CD8 Tfc maintain lytic capacity via CD107a and TNFα but can also mediate a lytic environment as a population during autoimmune disease.

IL-2-KO CD8 Tfc also transcribe genes associated with CD4 Tfh function (Fig. 4) and can promote IgG class switch in vitro (10). To evaluate mechanisms by which CD8 Tfc promote antibody class switch we measured cytokines associated with germinal center reactions. A majority of CD8 Tfc and non Tfc produce IFNγ, a cytokine that drives autoimmunity in this autoimmune model (56). IL-2-KO CD8 Tfc produce elevated IL-4 and significantly more IL-21 and IL-17 relative to CD8 non Tfc (Figure 5C). In addition, similar to cytolytic protein production in IL-2-KO CD8 Tfc, Tfh-associated cytokines are significantly co-produced (4.77% double; 0.44% triple) compared to IL-2-KO non Tfc (0.51% double, 0.01% triple) (Fig. 5D). While IL-2-KO CD8 Tfc can co-produce IL-21 and IL-4 (3.40%), a greater frequency express IL-21 (3.16%) or IL-4 (20.0%) alone (Figure 5D). CD8 Tfc maintain functional diversity as a population producing somewhat different cytokines and cytolytic proteins in individual cells. Whether this represents different stages of differentiation and function or a limitation on detection remains unknown.

3.6. B cell class switch and AID induction directed by CD8 Tfc.

B cell responses to cytokine often initiate in the extrafollicular region of the B cell follicle for plasma cell development (42) followed by somatic hypermutation and B cell cycling within the germinal center (43). Since CD8 Tfc maintain broad effector cytokine production within the population and can be identified within the germinal center and follicle of IL-2-KO mice, we next assessed localization of IL-2-KO CD8 Tfc that maintained helper-like cytokine function within lymphoid tissue using immunofluorescence. Splenic tissue sections were stained for IL-21 and IL-4, and IgD and PNA to determine germinal center position (Fig 6A). Both IL-2-KO CD4 and CD8 T cells in the germinal center and follicle have a large and significant frequency of IL-4 and IL-21 non-producing cells (50.39 +/−15.03%, 29.49 +/−32.28%), suggesting that these cells are also producing other cytokines not examined here or are not producing cytokines (Fig 6B and 6C). However, similar populations of follicular and germinal center IL-2-KO CD4 T cells produced IL-4, IL-21, or the two in combination (Fig 6B), whereas germinal center and follicular IL-2-KO CD8 T cells primarily produced IL-4 alone (Fig 6C). Similar frequencies of IL-4+ CD8 T cells were

found in germinal center (49.27 +/−39.0%) and follicle (43.02 +/−15.29%) of IL-2-KO mice suggesting that CD8 T cells may mediate B cell help in both regions.

To assess the specific role of IL-2-KO CD8 Tfc produced cytokine on B cell responses, we evaluated AID induction in naïve B cells. First, to investigate the influence of IL-21, WT or IL-21R-KO B cells were stimulated using supernatant from activated IL-2-KO CD8 Tfc or CD4 Tfh then assessed for intracellular AID. As expected, the absence of IL-21 signaling in IL-21R-KO B cells prevented AID induction by CD4 Tfh produced IL-21. Conversely, CD8 Tfc produced cytokines prompted AID induction independent of IL-21 responsiveness in B cells (Fig 6D). Given that germinal center and follicular localized CD8 Tfc cells produced primarily IL-4, we next assessed the contribution of CD8 Tfc produced IL-4 on B cell function. IL-2-KO CD8 Tfc or CD4 Tfh activated supernatant with and without IL-4 was added to sorted WT naïve B cells. As with IL-21 signaling, CD4 Tfh produced IL-4 promoted AID induction in B cells. In contrast, when IL-4 was removed from CD8 Tfc cell supernatant, B cell expression of AID was significantly reduced (Fig 6E). This suggests that while IL-21 is a key cytokine for mediating CD4 Tfh function, it may not play as significant a role in CD8 Tfc function. Together these data demonstrate that CD8 Tfc mediate B cell responses, at least in part, via cytokine secretion within the germinal center.

4. Discussion

Together, these data demonstrated that CD8 Tfc comprise a functionally non-redundant subset of CXCR5+ CD8 Tfc in systemic autoimmune disease. CD8 Tfc develop in the absence of functional Tregs and expand in the context of lymphoproliferation. By transcriptional profile and protein expression, CD8 Tfc resemble CD4 Tfh cells. CD8 Tfc maintain significant effector cytokine levels to function as B cell helpers in germinal center and follicular reactions, although their role is not limited to CD4 Tfh activities. IL-2-KO CD8 Tfc acquire the capacity to produce helper cytokines including the co-expression of IL-21 and IL-4. However, CD8 Tfc maintain the capacity for cytolytic function and express granzyme B and TNFα, suggesting the potential for functional mechanisms that diverge from CD4 Tfh cells. Although gene profiling (Fig 4) indicates that IL-2-KO CD4 Tfh cells also acquire substantial cytotoxic gene expression perhaps due to reduced Tfregs in the absence of IL-2 (57).

While both IL-2-KO CD4 Tfh and CD8 Tfc promote cytokine-mediated B cell AID induction, CD8 Tfc do not utilize IL-21 to mediate B cell responses. This is in contrast to CD4 Tfh cells that utilize IL-21 for AID induction and antibody class switching (42). Instead CD8 Tfc may use IL-4 or combinatorial interactions to mediate B cell responses. It is possible that direct cell:cell interactions such as CD40L known to be elevated on CD8 Tfc or mechanisms unique to CD8 Tfc are responsible for CD8 Tfc helper activity (10). In this study we cannot rule out a role for IL-2-KO CD8 Tfc cytolytic responses in antibody generation or in driving autoimmunity. However, CD8 Tfc position coupled with cytokine production in the germinal center and follicle along with AID induction suggest a dominant helper-like role. A cytotoxic role for CD8 Tfc can also be imagined for promoting apoptosis within the affinity maturation process, although this has not been assessed in any models with CXCR5+ CD8 T cell. T cells interactions with B cells at the follicular border, begin

the germinal center reaction (20). CD8 Tfc localization within the follicle places these cells spatially within this interaction. IL-4+ CD8 Tfc localized throughout the follicle and germinal center suggest that CD8 Tfc may promote B cell activities in either location during autoimmune disease. Live imaging studies between CD8 Tfc and B cells is likely required to further illustrate functional interactions. The types of B cell activities that CD8 Tfc cells influence are not fully defined and may include regulating somatic mutation, memory development, short-lived or long-lived plasma cell differentiation, and movement within the germinal center. However, we know that CD8 T cells promote plasma cell differentiation and antibody class switch, but do not alter germinal center B cell numbers (10).

CD8 Tfc appear in multiple models of systemic autoimmune disease, including IL-2 sufficient autoimmunity, promoting the hypothesis that CD8 Tfc development is associated with Treg dysfunction and not IL-2 regulation. Yet, some questions remain regarding the contribution of Treg deficiency or IL-2 signaling to CD8 Tfc development. IL-2 inhibits CD4 Tfh cell differentiation via STAT5 (58, 59). Yet, when IL-2 is depleted in scurfy mice CD8 Tfc fail to expand but IL-2-KOxscurfy mice have an increased frequency of CD8 Tfc. This contradictory data can be explained, in part, by the lymphoproliferation exhibited by IL-2xscurfy (47) that is absent in IL-2 depleted scurfy. IL-2.IFNγ dKO and IL-2.CD28 dKO models further highlight the role of lymphoproliferation in CD8 Tfc expansion.

Typically, reduced IFNγ signaling in autoimmune disease prevents germinal center B and Tfh cell development and accumulation (49). The absence of IFNγ signaling similarly reduces the frequency of CD8 Tfc in IL-2.IFNγ dKO mice compared to IL-2-KO mice. However, despite this reduced frequency of IL-2.IFNγ dKO CD8 Tfc, lymphoproliferation leads to expanded CD8 Tfc total numbers similar to observations in IL-2-KO mice that cannot be recovered in lymphopenic IL-2.CD28 dKO mice. Impaired CD8 Tfc expansion in IL-2.CD28 dKO mice suggests that CD28 signals may be required for CD8 Tfc development as in CD4 Tfh development (48, 60). Together, this supports the hypothesis that Treg deficiency releases CD8 Tfc function while IL-2 deficiency promotes lymphoproliferation associated with CD8 Tfc expansion. As CD8 Tfc can still develop even in the absence of CD4 T cells, including Tregs, albeit much less than in the presence of CD4 cells, it reasons that alternative mechanisms may initiate CD8 Tfc differentiation. To fully clarify the role of Treg control on CD8 Tfc development additional studies are needed.

CD8 Tfc are an effector T cell population that is closely associated with late-stage autoimmune disease and present with lymphoproliferation, autoantibodies, systemic activation, germinal center development including SLE and autoimmune hemolytic anemia. As such CD8 Tfc represent a promising avenue for autoimmune treatment.

Supplementary Material

Refer to Web version on PubMed Central for supplementary material.

Acknowledgements:

The authors thank Roy Hoglund, Emily Slocum and the staff members of the UC Merced Department of Animal Research Services for animal husbandry care, the UC Merced Stem Cell Instrumentation Foundry (SCIF) for their

assistance in cell sorting, Anand Subramaniam and the UC Merced Imaging and Microscopy Facility for assistance and use of microscopy equipment, Hans Dooms from Boston University for providing NOD mouse tissues, Anh Diep and Christi Waer for experimental assistance and evaluation of the manuscript, and undergraduate research assistant Nicole Quiroz-Lumbe.

Funding:

This work was supported by the National Institutes of Health Grant R00HL090706 and R15HL146779 to K.K.H., the 2019 University of California Presidential Dissertation Year Fellowship to K.M.V., and the University of California. The Zeiss LSM 880 microscope used for imaging was purchased by NSF grant DMR-1625733. L.W.S. is a Student Success Intern funded by the University of California Office of the President in support of Student Success initiatives jointly implemented by the Division of Student Affairs and the Office of Undergraduate Education at University of California, Merced.

Abbreviations:

CD8 Tfc	CD8 T follicular cells
CD4 Tfh	CD4 T follicular cells
Treg	T regulatory cells
scurfy	BALB/c hemizygous male Foxp3sf/Y
IL-2Rα	IL-2 receptor alpha
KO	knock-out
dKO	double knock-out
Mrl.lpr	MRL/MpJ-*Fas*^{lpr}/J
Tfreg	T follicular regulatory cell

References:

1. Valentine KM, and Hoyer KK. 2019. CXCR5+ CD8 T Cells: Protective or Pathogenic? Front Immunol 10: 1322. [PubMed: 31275308]
2. Yu D, and Ye L. 2018. A Portrait of CXCR5 Follicular Cytotoxic CD8 T cells. Trends Immunol 39: 965–979. [PubMed: 30377045]
3. Fousteri G, and Kuka M. 2020. The elusive identity of CXCR5 CD8 T cell in viral infection and autoimmunity: Cytotoxic, regulatory, or helper cells? Mol Immunol 119: 101–105. [PubMed: 32007752]
4. Petrovas C, Ferrando-Martinez S, Gerner MY, Casazza JP, Pegu A, Deleage C, Cooper A, Hataye J, Andrews S, Ambrozak D, Del Rio Estrada PM, Boritz E, Paris R, Moysi E, Boswell KL, Ruiz-Mateos E, Vagios I, Leal M, Ablanedo-Terrazas Y, Rivero A, Gonzalez-Hernandez LA, McDermott AB, Moir S, Reyes-Teran G, Docobo F, Pantaleo G, Douek DC, Betts MR, Estes JD, Germain RN, Mascola JR, and Koup RA. 2017. Follicular CD8 T cells accumulate in HIV infection and can kill infected cells in vitro via bispecific antibodies. Science translational medicine 9.
5. Quigley MF, Gonzalez VD, Granath A, Andersson J, and Sandberg JK. 2007. CXCR5+ CCR7- CD8 T cells are early effector memory cells that infiltrate tonsil B cell follicles. European journal of immunology 37: 3352–3362. [PubMed: 18000950]
6. Hardtke S, Ohl L, and Forster R. 2005. Balanced expression of CXCR5 and CCR7 on follicular T helper cells determines their transient positioning to lymph node follicles and is essential for efficient B-cell help. Blood 106: 1924–1931. [PubMed: 15899919]
7. Im SJ, Hashimoto M, Gerner MY, Lee J, Kissick HT, Burger MC, Shan Q, Hale JS, Nasti TH, Sharpe AH, Freeman GJ, Germain RN, Nakaya HI, Xue HH, and Ahmed R. 2016. Defining CD8+

T cells that provide the proliferative burst after PD-1 therapy. Nature 537: 417–421. [PubMed: 27501248]

8. Mylvaganam GH, Rios D, Abdelaal HM, Iyer S, Tharp G, Mavigner M, Hicks S, Chahroudi A, Ahmed R, Bosinger SE, Williams IR, Skinner PJ, Velu V, and Amara RR. 2017. Dynamics of SIV-specific CXCR5+ CD8 T cells during chronic SIV infection. Proc Natl Acad Sci U S A 114: 1976–1981. [PubMed: 28159893]
9. Xing J, Zhang C, Yang X, Wang S, Wang Z, Li X, and Yu E. 2017. CXCR5(+)CD8(+) T cells infiltrate the colorectal tumors and nearby lymph nodes, and are associated with enhanced IgG response in B cells. Exp Cell Res.
10. Valentine KM, Davini D, Lawrence TJ, Mullins GN, Manansala M, Al-Kuhlani M, Pinney JM, Davis JK, Beaudin AE, Sindi SS, Gravano DM, and Hoyer KK. 2018. CD8 Follicular T Cells Promote B Cell Antibody Class Switch in Autoimmune Disease. J Immunol 201: 31–40. [PubMed: 29743314]
11. Le KS, Amé-Thomas P, Tarte K, Gondois-Rey F, Granjeaud S, Orlanducci F, Foucher ED, Broussais F, Bouabdallah R, Fest T, Leroux D, Yadavilli S, Mayes PA, Xerri L, and Olive D. 2018. CXCR5 and ICOS expression identifies a CD8 T-cell subset with T. Blood Adv 2: 1889–1900. [PubMed: 30087107]
12. Chen Y, Yu M, Zheng Y, Fu G, Xin G, Zhu W, Luo L, Burns R, Li QZ, Dent AL, Zhu N, Cui W, Malherbe L, Wen R, and Wang D. 2019. CXCR5+ PD-1+ follicular helper CD8 T cells control B cell tolerance. Nat Commun 10: 4415. [PubMed: 31562329]
13. Leong YA, Chen Y, Ong HS, Wu D, Man K, Deleage C, Minnich M, Meckiff BJ, Wei Y, Hou Z, Zotos D, Fenix KA, Atnerkar A, Preston S, Chipman JG, Beilman GJ, Allison CC, Sun L, Wang P, Xu J, Toe JG, Lu HK, Tao Y, Palendira U, Dent AL, Landay AL, Pellegrini M, Comerford I, McColl SR, Schacker TW, Long HM, Estes JD, Busslinger M, Belz GT, Lewin SR, Kallies A, and Yu D. 2016. CXCR5(+) follicular cytotoxic T cells control viral infection in B cell follicles. Nature immunology 17: 1187–1196. [PubMed: 27487330]
14. Nurieva RI, Chung Y, Martinez GJ, Yang XO, Tanaka S, Matskevitch TD, Wang YH, and Dong C. 2009. Bcl6 mediates the development of T follicular helper cells. Science 325: 1001–1005. [PubMed: 19628815]
15. Johnston RJ, Poholek AC, DiToro D, Yusuf I, Eto D, Barnett B, Dent AL, Craft J, and Crotty S. 2009. Bcl6 and Blimp-1 are reciprocal and antagonistic regulators of T follicular helper cell differentiation. Science 325: 1006–1010. [PubMed: 19608860]
16. Yu D, Rao S, Tsai LM, Lee SK, He Y, Sutcliffe EL, Srivastava M, Linterman M, Zheng L, Simpson N, Ellyard JI, Parish IA, Ma CS, Li QJ, Parish CR, Mackay CR, and Vinuesa CG. 2009. The transcriptional repressor Bcl-6 directs T follicular helper cell lineage commitment. Immunity 31: 457–468. [PubMed: 19631565]
17. He R, Hou S, Liu C, Zhang A, Bai Q, Han M, Yang Y, Wei G, Shen T, Yang X, Xu L, Chen X, Hao Y, Wang P, Zhu C, Ou J, Liang H, Ni T, Zhang X, Zhou X, Deng K, Chen Y, Luo Y, Xu J, Qi H, Wu Y, and Ye L. 2016. Follicular CXCR5-expressing CD8+ T cells curtail chronic viral infection. Nature 537: 412–428. [PubMed: 27501245]
18. Jin Y, Lang C, Tang J, Geng J, Song HK, Sun Z, and Wang J. 2017. CXCR5(+)CD8(+) T cells could induce the death of tumor cells in HBV-related hepatocellular carcinoma. International immunopharmacology 53: 42–48. [PubMed: 29032029]
19. Ye L, Li Y, Tang H, Liu W, Chen Y, Dai T, Liang R, Shi M, Yi S, Chen G, and Yang Y. 2019. CD8+CXCR5+T cells infiltrating hepatocellular carcinomas are activated and predictive of a better prognosis. Aging (Albany NY) 11: 8879–8891. [PubMed: 31663864]
20. Crotty S 2014. T follicular helper cell differentiation, function, and roles in disease. Immunity 41: 529–542. [PubMed: 25367570]
21. Crotty S 2011. Follicular helper CD4 T cells (TFH). Annual review of immunology 29: 621–663.
22. Hoyer KK, Wolslegel K, Dooms H, and Abbas AK. 2007. Targeting T cell-specific costimulators and growth factors in a model of autoimmune hemolytic anemia. J Immunol 179: 2844–2850. [PubMed: 17709498]

23. Mullins GN, Valentine KM, Al-Kuhlani M, Davini D, Jensen KDC, and Hoyer KK. 2020. T cell signaling and Treg dysfunction correlate to disease kinetics in IL-2Rα-KO autoimmune mice. Scientific reports 10: 21994. [PubMed: 33319815]
24. Rosloniec EF, Cremer M, Kang AH, Myers LK, and Brand DD. 2010. Collagen-induced arthritis. Current protocols in immunology Chapter 15: Unit 15.15.11–25.
25. Bolger AM, Lohse M, and Usadel B. 2014. Trimmomatic: a flexible trimmer for Illumina sequence data. Bioinformatics 30: 2114–2120. [PubMed: 24695404]
26. Liao Y, Smyth GK, and Shi W. 2019. The R package Rsubread is easier, faster, cheaper and better for alignment and quantification of RNA sequencing reads. Nucleic Acids Res 47: e47. [PubMed: 30783653]
27. Liao Y, Smyth GK, and Shi W. 2014. featureCounts: an efficient general purpose program for assigning sequence reads to genomic features. Bioinformatics 30: 923–930. [PubMed: 24227677]
28. Robinson MD, McCarthy DJ, and Smyth GK. 2010. edgeR: a Bioconductor package for differential expression analysis of digital gene expression data. Bioinformatics 26: 139–140. [PubMed: 19910308]
29. Ritchie ME, Phipson B, Wu D, Hu Y, Law CW, Shi W, and Smyth GK. 2015. limma powers differential expression analyses for RNA-sequencing and microarray studies. Nucleic Acids Res 43: e47. [PubMed: 25605792]
30. Liu R, Holik AZ, Su S, Jansz N, Chen K, Leong HS, Blewitt ME, Asselin-Labat ML, Smyth GK, and Ritchie ME. 2015. Why weight? Modelling sample and observational level variability improves power in RNA-seq analyses. Nucleic Acids Res 43: e97. [PubMed: 25925576]
31. Law CW, Chen Y, Shi W, and Smyth GK. 2014. voom: Precision weights unlock linear model analysis tools for RNA-seq read counts. Genome Biol 15: R29. [PubMed: 24485249]
32. Benjamini Y, and Hochberg Y. 1995. Controlling the False Discovery Rate: A Practical and Powerful Approach to Multiple Testing. Journal of the Royal Statistical Society. Series B (Methodological) 57: 289–300.
33. Kolde R 2019. pheatmap: Pretty Heatmaps. 1.0.12 ed.
34. Yu G, Wang LG, Han Y, and He QY. 2012. clusterProfiler: an R package for comparing biological themes among gene clusters. OMICS 16: 284–287. [PubMed: 22455463]
35. Carlson M 2019. org.Mm.eg.db: Genome wide annotation for Mouse.
36. Team, R. C. 2019. R: A Language and Environment for Statistical Computing. R Foundation for Statistical Computing, Vienna, Austria.
37. Wickham H, Averick M, Bryan J, Chang W, McGowan LDA, François R, Grolemund G, Hayes A, Henry L, Hester J, Kuhn M, Pedersen TL, Miller E, Bache SM, Müller K, Ooms J, Robinson D, Seidel DP, Spinu V, Takahashi K, Vaughan D, Wilke C, Woo K, and Yutani H. 2019. Welcome to the tidyverse. Journal of Open Source Software 4: 1686.
38. Ding Y, Mountz JD, and Hsu HC. 2015. Identification of follicular T helper cells in tissue sections. Methods Mol Biol 1291: 13–25. [PubMed: 25836298]
39. Elsner RA, Ernst DN, and Baumgarth N. 2012. Single and coexpression of CXCR4 and CXCR5 identifies CD4 T helper cells in distinct lymph node niches during influenza virus infection. J Virol 86: 7146–7157. [PubMed: 22532671]
40. Whiteland JL, Shimeld C, Nicholls SM, Easty DL, Williams NA, and Hill TJ. 1997. Immunohistochemical detection of cytokines in paraffin-embedded mouse tissues. J Immunol Methods 210: 103–108. [PubMed: 9502589]
41. Yang X, Yang J, Chu Y, Wang J, Guan M, Zhu X, Xue Y, and Zou H. 2013. T follicular helper cells mediate expansion of regulatory B cells via IL-21 in Lupus-prone MRL/lpr mice. PLoS One 8: e62855. [PubMed: 23638156]
42. Odegard JM, Marks BR, DiPlacido LD, Poholek AC, Kono DH, Dong C, Flavell RA, and Craft J. 2008. ICOS-dependent extrafollicular helper T cells elicit IgG production via IL-21 in systemic autoimmunity. J Exp Med 205: 2873–2886. [PubMed: 18981236]
43. Mesin L, Ersching J, and Victora GD. 2016. Germinal Center B Cell Dynamics. Immunity 45: 471–482. [PubMed: 27653600]
44. Rankin AL, Guay H, Herber D, Bertino SA, Duzanski TA, Carrier Y, Keegan S, Senices M, Stedman N, Ryan M, Bloom L, Medley Q, Collins M, Nickerson-Nutter C, Craft J, Young D,

and Dunussi-Joannopoulos K. 2012. IL-21 receptor is required for the systemic accumulation of activated B and T lymphocytes in MRL/MpJ-Fas(lpr/lpr)/J mice. J Immunol 188: 1656–1667. [PubMed: 22231702]

45. DiToro D, Winstead CJ, Pham D, Witte S, Andargachew R, Singer JR, Wilson CG, Zindl CL, Luther RJ, Silberger DJ, Weaver BT, Kolawole EM, Martinez RJ, Turner H, Hatton RD, Moon JJ, Way SS, Evavold BD, and Weaver CT. 2018. Differential IL-2 expression defines developmental fates of follicular versus nonfollicular helper T cells. Science 361.
46. Papillion A, Powell MD, Chisolm DA, Bachus H, Fuller MJ, Weinmann AS, Villarino A, O'Shea JJ, León B, Oestreich KJ, and Ballesteros-Tato A. 2019. Inhibition of IL-2 responsiveness by IL-6 is required for the generation of GC-T(FH) cells. Science immunology 4.
47. Zheng L, Sharma R, Gaskin F, Fu SM, and Ju ST. 2007. A novel role of IL-2 in organ-specific autoimmune inflammation beyond regulatory T cell checkpoint: both IL-2 knockout and Fas mutation prolong lifespan of Scurfy mice but by different mechanisms. J Immunol 179: 8035–8041. [PubMed: 18056343]
48. Linterman MA, Rigby RJ, Wong R, Silva D, Withers D, Anderson G, Verma NK, Brink R, Hutloff A, Goodnow CC, and Vinuesa CG. 2009. Roquin differentiates the specialized functions of duplicated T cell costimulatory receptor genes CD28 and ICOS. Immunity 30: 228–241. [PubMed: 19217324]
49. Lee SK, Silva DG, Martin JL, Pratama A, Hu X, Chang PP, Walters G, and Vinuesa CG. 2012. Interferon-gamma excess leads to pathogenic accumulation of follicular helper T cells and germinal centers. Immunity 37: 880–892. [PubMed: 23159227]
50. Kim H-J, Verbinnen B, Tang X, Lu L, and Cantor H. 2010. Inhibition of follicular T-helper cells by CD8+ regulatory T cells is essential for self tolerance. Nature 467: 328–332. [PubMed: 20844537]
51. Churlaud G, Pitoiset F, Jebbawi F, Lorenzon R, Bellier B, Rosenzwajg M, and Klatzmann D. 2015. Human and Mouse CD8(+)CD25(+)FOXP3(+) Regulatory T Cells at Steady State and during Interleukin-2 Therapy. Front Immunol 6: 171. [PubMed: 25926835]
52. Akimova T, Beier UH, Wang L, Levine MH, and Hancock WW. 2011. Helios expression is a marker of T cell activation and proliferation. PLoS One 6: e24226. [PubMed: 21918685]
53. Kim HJ, Barnitz RA, Kreslavsky T, Brown FD, Moffett H, Lemieux ME, Kaygusuz Y, Meissner T, Holderried TA, Chan S, Kastner P, Haining WN, and Cantor H. 2015. Stable inhibitory activity of regulatory T cells requires the transcription factor Helios. Science 350: 334–339. [PubMed: 26472910]
54. Rahman MA, McKinnon KM, Karpova TS, Ball DA, Venzon DJ, Fan W, Kang G, Li Q, and Robert-Guroff M. 2018. Associations of Simian Immunodeficiency Virus (SIV)-Specific Follicular CD8(+) T Cells with Other Follicular T Cells Suggest Complex Contributions to SIV Viremia Control. J Immunol 200: 2714–2726. [PubMed: 29507105]
55. Tang J, Zha J, Guo X, Shi P, and Xu B. 2017. CXCR5(+)CD8(+) T cells present elevated capacity in mediating cytotoxicity toward autologous tumor cells through interleukin 10 in diffuse large B-cell lymphoma. International immunopharmacology 50: 146–151. [PubMed: 28662433]
56. Hoyer KK, Kuswanto WF, Gallo E, and Abbas AK. 2009. Distinct roles of helper T-cell subsets in a systemic autoimmune disease. Blood 113: 389–395. [PubMed: 18815283]
57. Xie MM, Fang S, Chen Q, Liu H, Wan J, and Dent AL. 2019. Follicular regulatory T cells inhibit the development of granzyme B-expressing follicular helper T cells. JCI insight 4.
58. Ballesteros-Tato A, Leon B, Graf BA, Moquin A, Adams PS, Lund FE, and Randall TD. 2012. Interleukin-2 inhibits germinal center formation by limiting T follicular helper cell differentiation. Immunity 36: 847–856. [PubMed: 22464171]
59. Johnston RJ, Choi YS, Diamond JA, Yang JA, and Crotty S. 2012. STAT5 is a potent negative regulator of TFH cell differentiation. J Exp Med 209: 243–250. [PubMed: 22271576]
60. Gigoux M, Shang J, Pak Y, Xu M, Choe J, Mak TW, and Suh WK. 2009. Inducible costimulator promotes helper T-cell differentiation through phosphoinositide 3-kinase. Proc Natl Acad Sci U S A 106: 20371–20376. [PubMed: 19915142]

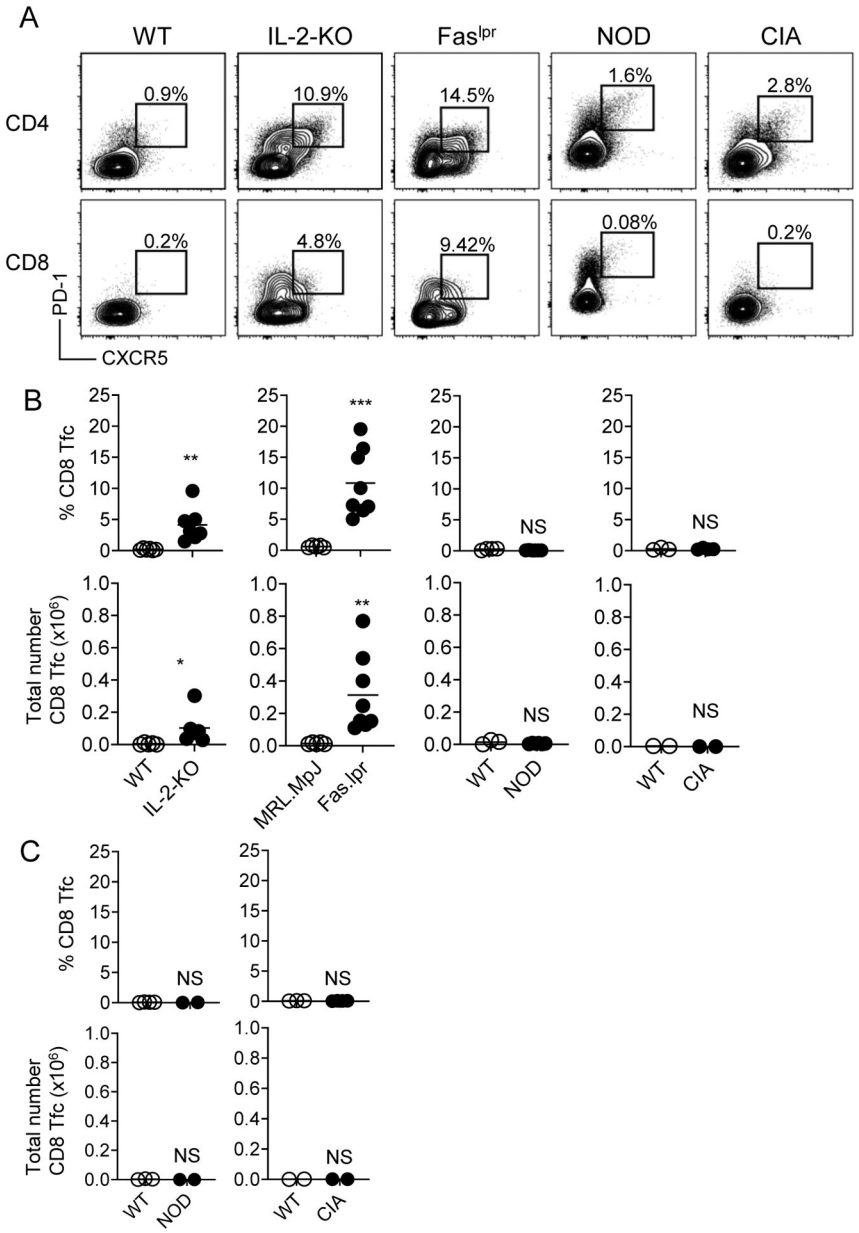

Fig 1. CD8 Tfc arise in multiple models of autoimmune disease.

(**A**) Representative flow plots compare CXCR5 and PD-1 expression on live B220^{-}CD11c^{-}CD11b^{-}GR-1^{-}. CD4 or CD8 T cells from spleens of 17–21-day old IL-2-KO and WT littermate controls, 17–23-week old Fas^{lpr} and MRL.MpJ controls, 11 week old diseased (urine-glucose positive) NOD and 6–14-week old WT controls, and 7-week post-induction CIA and PBS control mice. (**B**) Frequency and total number of CD8 Tfc in the indicated model is shown. (**C**) The frequency and total number of CD8 Tfc isolated from the draining lymph nodes of NOD and CIA mouse models is shown. Each symbol indicates an individual animal. Data representative of 1–3 independent experiments per comparison. Statistics: unpaired one-tailed Student's t-test relative to indicated controls with a Welch correction if necessary. NS= not significant, * $p<0.05$, ** $p<0.01$, *** $p\leq0.001$.

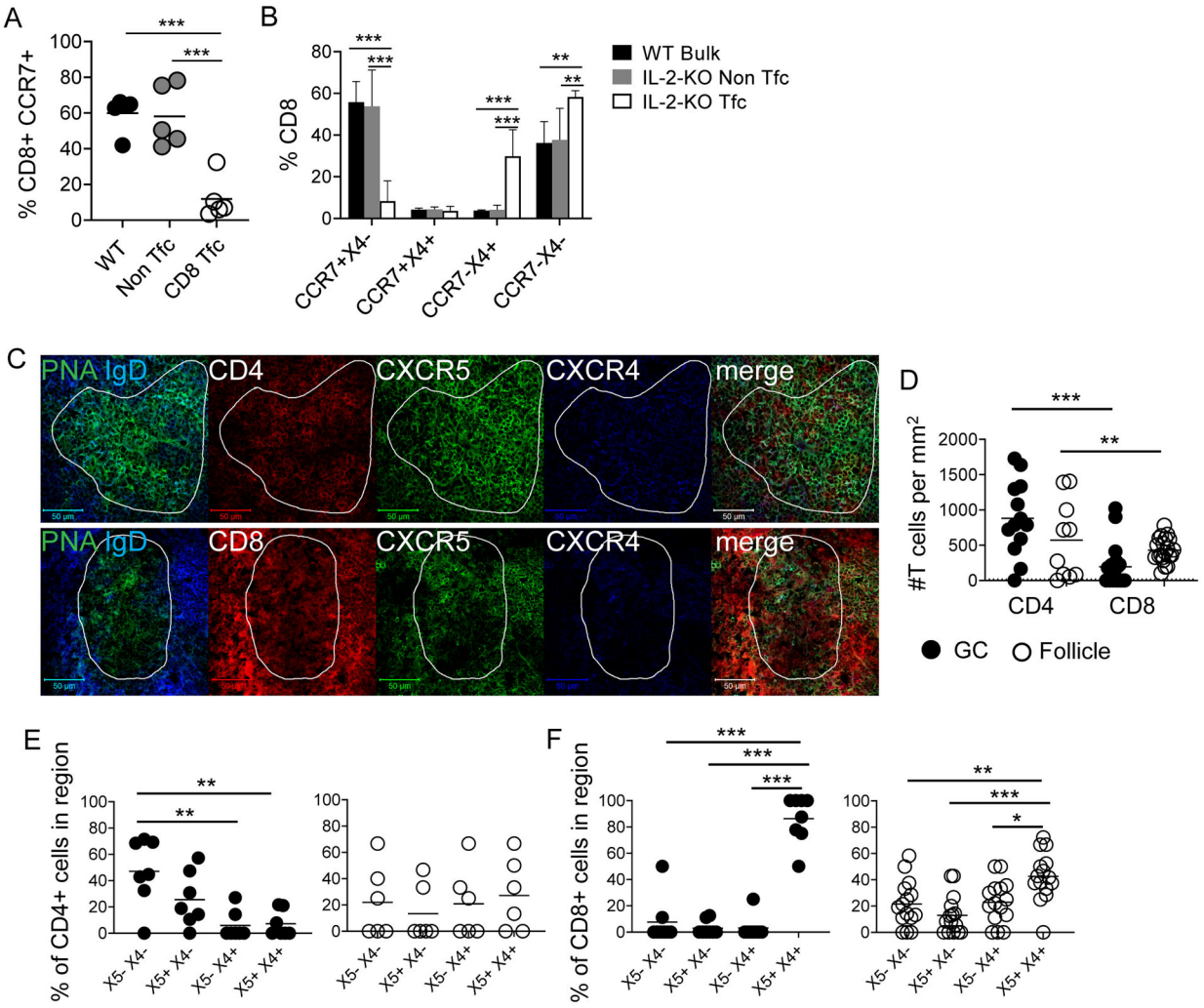

Fig 2. CD8 Tfc localize to GC and follicle.

(**A, B**) Splenocytes from 17–21-day old IL-2-KO and WT littermate controls were stained to identify CD8 Tfc. (**A**) The frequency of CCR7+ or (**B**) the mean frequency of CCR7 and CXCR4 (X4) co-expression ± SD was analyzed on bulk WT CD8, IL-2-KO non Tfc and IL-2-KO CD8 Tfc. (**C**) Representative images of 19–21-day old IL-2-KO spleen sections that were stained for CXCR5, CXCR4, PNA, IgD, and CD4 or CD8. The outlined germinal center was defined as high PNA and low IgD are shown. (**D**) Quantification of CD4 or CD8 T cells counted in immunofluorescence images at 40x asper mm^2 of the counting area. (**E**) Frequency of CD4 or (**F**) CD8 T cells co-expressing CXCR5 and CXCR4 within the germinal center (filled circle) or follicle (open circle). Data representative of 3–4 independent experiments. (A, D-F) Each symbol indicates an individual animal. Statistics: (A, D-F) 1-way ANOVA with multiple comparisons and Bonferroni correction, (B) 2-way ANOVA with multiple comparisons and Bonferroni correction. * $p<0.05$, ** $p<0.01$, *** $p\leq0.001$.

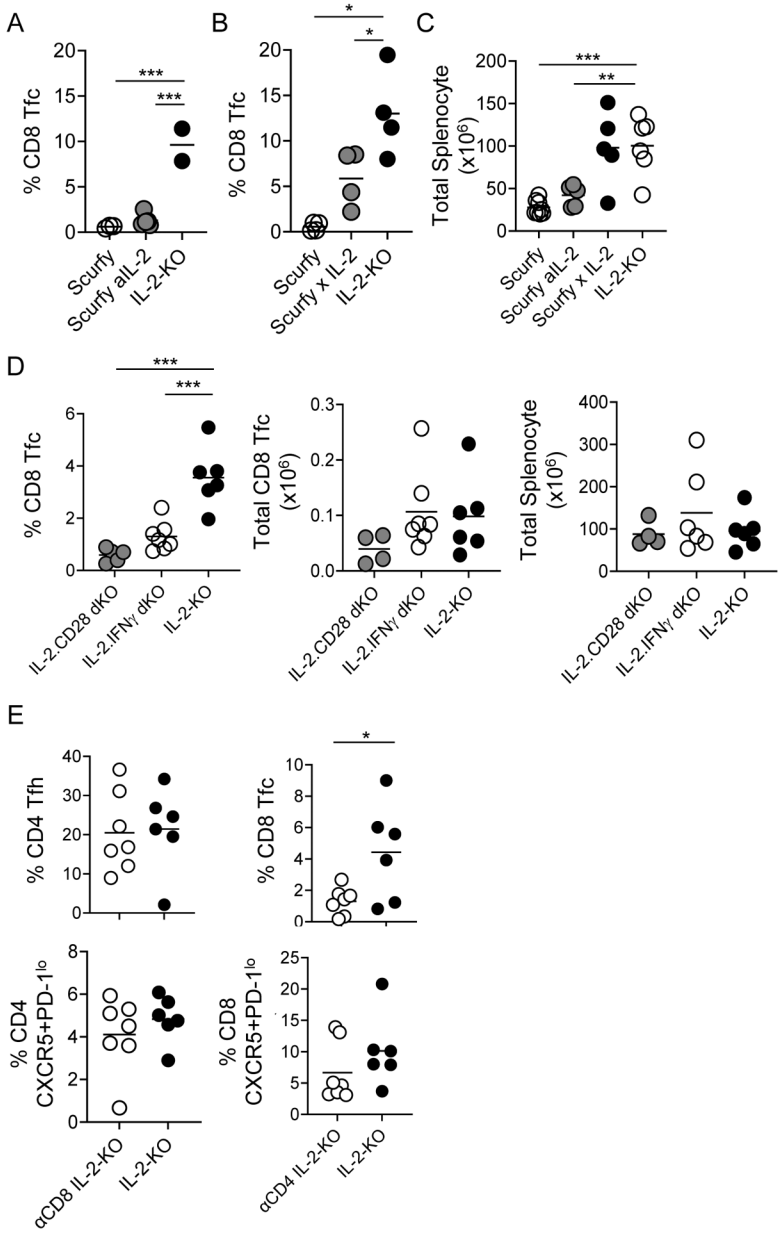

Fig 3. T cell regulation controls CD8 Tfc differentiation.

Splenic CD8 Tfc frequencies were compared between (**A**) 17–21-day old IL-2-KO, 16–21-day old scurfy mice treated 5 times with PBS (scurfy) and anti-IL-2 (scurfy aIL-2) or(**B**) 18–20-day old IL-2-KO, scurfy, and scurfyxIl-2-KO (ScurfyxIl-2) mice. (**C**) Total splenocyte number in scurfy, scurfy aIL-2, ScurfyxIl-2, and IL-2-KO mice described in A and B. (**D**) The frequency and total number of splenic CD8 Tfc cells or total number of splenocytes was compared between 18–21-day old IL-2-KO, 12-week old IL-2.CD28 dKO and 12-week old IL-2.IFNγ dKO mice. (**E**) IL-2-KO mice were treated 5 times with anti-CD4 or anti-CD8 between 8–16-days of age to deplete either CD4 or CD8 T cells. The frequency and total number of CD4 Tfh and CD4 CXCR5+PD-1^{lo} in the absence of CD8 T cells or CD8 Tfc and CD8 CXCR5+PD-1^{lo} in the absence of CD4 T cell was compared to PBS-treated

IL-2-KO mice. Each symbol indicates an individual animal. Data representative of 2–4 independent. Statistics: (A-D) 1-way ANOVA with multiple comparisons and Bonferroni correction. (E) unpaired Student's t-test with a Welch correction. * $p<0.05$, ** $p<0.01$, *** $p\leq0.001$.

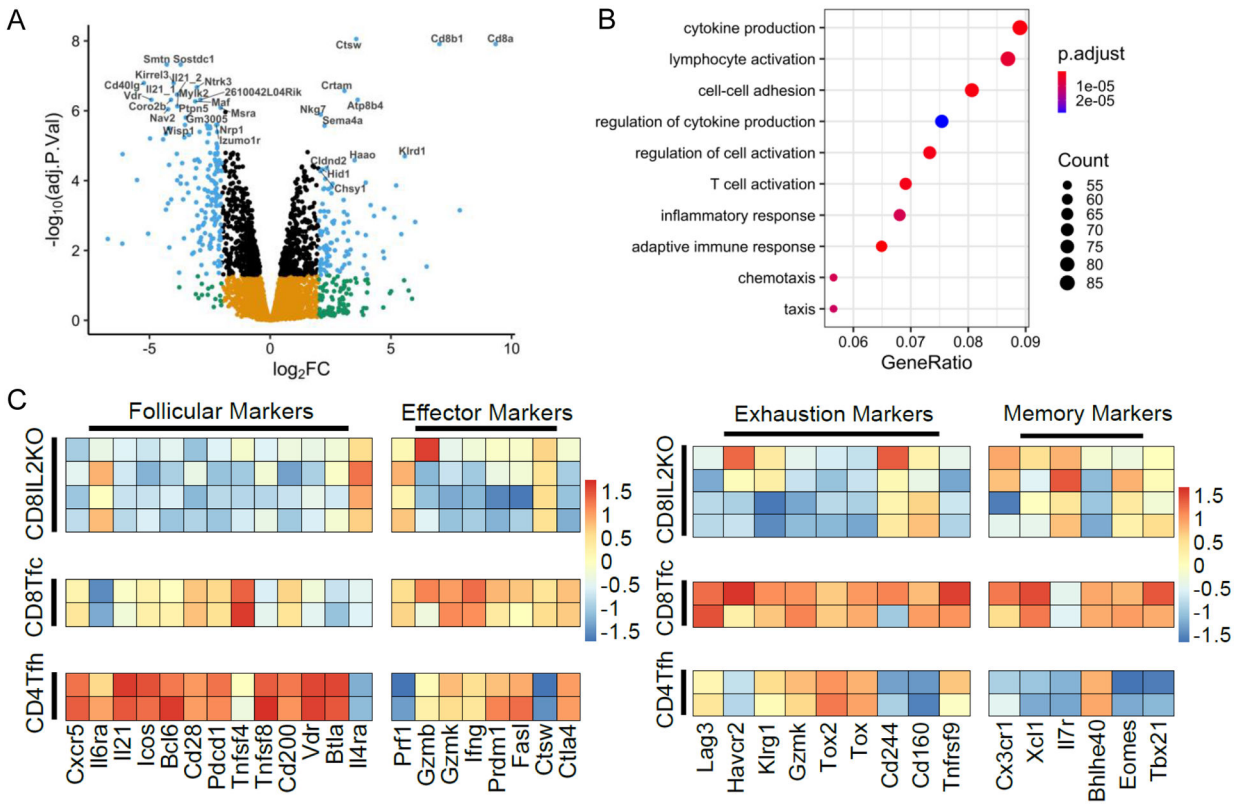

Fig 4. CD8 Tfc transcriptional profiling highlights a diverse helper-like and memory phenotype.

RNAseq of 2 independent IL-2-KO CD4 Tfh and CD8 Tfc from 6–7 pooled lymph nodes and Spleens. (**A**) Volcano plot of differential expression defined as log fold change (LFC) of IL-2-KO CD8 Tfc vs IL-2-KO CD4 Tfh with 479 upregulated and 639 downregulated genes. (**B**) Gene Ontology plot of top 10 categories. X-axis shows the gene ratio which indicates the quantity of genes present from each category divided by total number of differentially expressed genes. (**C**) Heatmaps containing normalized gene expression (Log-CPM) marked by different gene class. Cell type is defined as the first column labeled “CellType” of the heatmap, marker type is defined as “Gene.Class” as the first row at the top.

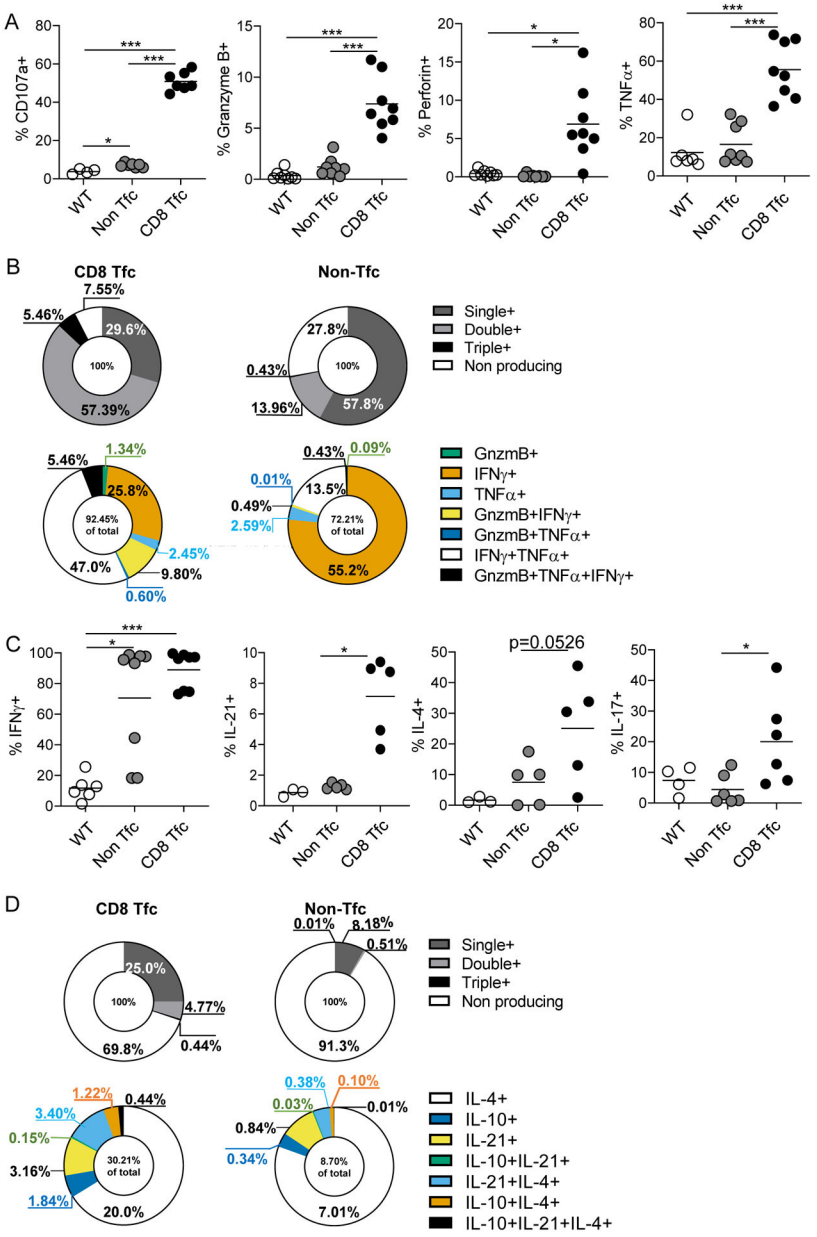

Fig 5. CD8 Tfc maintain diverse functional capacity.

IL-2-KO and WT lymphocytes were stimulated with PMA and ionomycin with BFA for 5 hours, then analyzed for cytokine expression in WT naïve CD8 T, IL-2-KO CD8 non Tfc and IL-2-KO CD8 Tfc populations. (**A**) Frequency of cytokine expressing cells and mean fluorescence intensity of (MFI) of CD107a, Granzyme B, Perforin and TNFα. (**B**) Pie charts illustrate polyfunctional cytolytic protein expression by IL-2-KO CD8 Tfc and non CD8 Tfc. Grey scale figures show non-producing, single, double and triple expression of the total population. Color figures show expression of Granzyme B, IFNγ and/or TNFα as a percentage of the cytokine expressing population defined. (**C**) Frequency of cytokine expressing cells and MFI of IFNγ, IL-21, IL-4, and IL-17. (**D**) Pie charts illustrate polyfunctional Tfh-associated protein expression by IL-2-KO CD8 Tfc and non CD8 Tfc.

Grey scale figures show non-producing, single, double and triple expression of the total population. Color figures show expression of IL-4, IL-10 and/or IL-21 as a percentage of the cytokine expressing population defined. Each symbol indicates an individual animal. Data representative of 3–6 independent experiments. Statistics: (A, C) 1-way ANOVA with multiple comparisons of matched pairs and Bonferroni correction. * $p<0.05$, *** $p\leq0.001$.

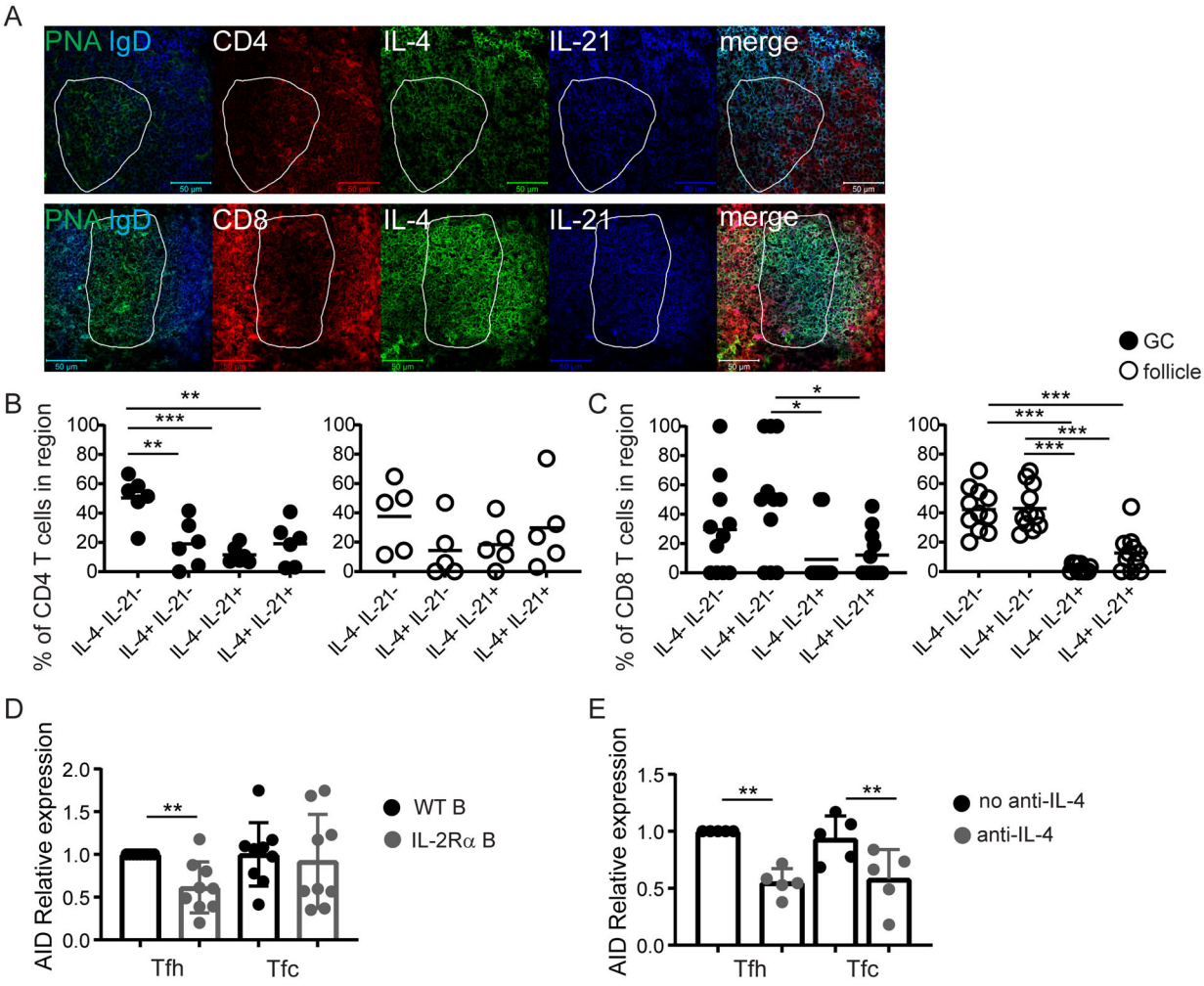

Fig 6. CD8 Tfc produce IL-4 and IL-21 within GC and follicle.

(**A**) IL-2-KO spleen sections were stained for IL-4, IL-21, PNA, IgD, and CD4 or CD8. Region outlined is the germinal center, defined by high PNA and low IgD. (**B, C**) Frequency of (B) CD4 or (C) CD8 T cells expressing IL-4 and/or IL-21 of total CD4 or CD8 T cells counted within the given region. (**D, E**) Sorted IL-2-KO CD4 Tfh and CD8 Tfc were stimulated for 3 days with anti-CD3 and anti-CD28, with (E) or without (D) neutralizing anti-IL-4. T cell supernatant was then plated with B cells and anti-IgM and anti-CD40 for 3 days. B cells were then collected and assessed for AID expression by flow cytometry. MFI for each experiment was normalized to Tfh with WT B cells, setting that condition to 1. Data representative of 4 experiments with a total n of 4 per group for D and n of 5–8 per group for C-D. Statistics (D, E) paired Student's t-test, (B-C) one-way ANOVA with multiple comparisons and Bonferroni correction. * $p<0.05$, ** $p<0.01$, *** $p\leq0.001$.